The first photometric investigation of the contact binary OQ Cam

Ya-Ni Guo (郭雅妮)[1], Kai Li (李凯)[1,2], Qi-Qi Xia (夏琪琪)[1], Xing Gao (高兴)[2], Lin-Qiao Jiang
(江林巧)[3] and Yuan Liu (刘媛)[4]

[1] Shandong Key Laboratory of Optical Astronomy and Solar-Terrestrial Environment, School of Space Science and Physics, Institute of Space Sciences, Shandong University, Weihai 264209, China; *kaili@sdu.edu.cn*

[2] Xinjiang Astronomical Observatory, Urumqi 830011, China

[3] Artificial Intelligence Key Laboratory of Sichuan Province, Sichuan University of Science & Engineering, Zigong 643000, China

[4] Qilu Institute of Technology, Jinan 250200, China

Abstract The first charge-coupled device photometric light curves in B, V, R_c, and I_c bands of the short-period contact binary star OQ Cam are presented. Through analyzing the light curves with the Wilson-Devinney code, it is found that OQ Cam is a W-type shallow contact binary star with a contact degree of $f = 20.2\%$. Based on the $O - C$ analyzing, the orbit period displays a long term increasing with a rate of $dP/dt = 4.40 \times 10^{-7}$ d yr^{-1}. The increasing in orbit period can be interpreted by mass transfer from the less massive component to the more massive one. As the orbit period increases, OQ Cam would evolve from the present shallow contact configuration to a non-contact stage. So it may be a potential candidate to confirm the thermal relaxation oscillation theory.

Key words: stars: binaries: close — stars: binaries: eclipsing — stars: evolution — stars: individual (OQ Cam)

1 INTRODUCTION

In the Milky Way, almost half of the stars are binary stars. The main characteristics of EW-type binaries are that primary minimum is almost as deep as the secondary minimum of the light curve, their orbital periods are frequently shorter than one day and two components have mass transfer (He et al. 2016). Normally, EW-type binary stars are contact binary systems, which refer to both two components filling their Roche Lobes. The two component stars have a common convection envelope, located between the inner and outer critical surfaces of the Roche model. They frequently have mass transfer through inner Lagrangian point. The two components have close surface temperatures (Qian et al. 2014, 2017). The mass transfer has a great influence on the evolution of the close binary systems. It would change the mass distributions of binary systems, further leading to variations of the orbital periods. There are several other reasons for the long-term variations of orbital period: mass loss from the binary system, which makes the period decreasing; angular momentum loss (AML) from the binary system via a magnetic

stellar wind or by the third body removing the angular momentum from the central system, which permanently makes the period decreasing; and the common convective envelope (CCE) dominated mechanism. This mechanism is especially applied to high mass ratios. The variation of orbit period depends on the fill-out factor that is regarded as a measurement of the thickness of CCE (Liu et al. 2018; Zhao et al. 2014). The third body has a significant effect on the evolution of binary system. Generally speaking, the presence of a third body will lead to stellar mergers, X-ray binaries, gamma-ray bursts and so on (Zhao et al. 2014). Through the investigation of eclipsing binary stars, many parameters can be determined for example the orbit period variation, mass, temperature, radius, luminosity and so on. According to a large number of observations, there is a popular belief that contact binary stars are mainly formed from detached or semi-detached binary stars with cool components, and they will evolve into rapidly rotating single stars (Roxburgh 1965; Bradstreet & Guinan 1994; Stepień 2006). The evolution of contact binary relies on the angular momentum left in the system, mass transfer rate and angular momentum loss rate. Some typical

contact binary evolutions are presented by Stepień (2006); Stepień & Gazeas (2012). However, this conclusion is still under debate at present and further research is still needed, so we have to study more contact binaries.

Thermal relaxation oscillation theory (Lucy 1976; Flannery 1976; Robertson & Eggleton 1977) is an important model for the structure and evolution of marginal contact binary stars. This theory includes two phases: during contact phase, mass is transferred from the less massive component to the more massive component; while during the non-contact phase, mass is returned to the less massive component. With the increasing of the period, the shallow contact binary stars may evolve from contact phase into non-contact phase. Contact binary stars are divided into W-type systems and A-type ones. If the more massive component is hotter, the binary star is an A-type binary star. If the more massive component is cooler, the binary star is a W-type binary star (Binnendijk 1970, 1977). Research has shown that when $q \geq 0.4$, there are more W-type binaries than A-type; $0.25 \leq q \leq 0.4$, there are an even distribution of W-type binaries and A-type ones; $q < 0.25$, the number of A-type binaries are more than W-type binaries (Kim et al. 2016). Zhang et al. (2020) has presented the secondary stars of A-type binaries are evolved from initial more massive stars, while the ones of W-type are formed via mass transfer. Some scientists believe that W-type binaries will evolve into A-type ones (Hilditch et al. 1989; Awadalla & Hanna 2005; Eker et al. 2006; Gazeas & Niarchos 2006) and someone believes that there is no evolutionary relationship between two types (Yildiz & Doğan 2013). This argument is under debate.

The eclipsing star OQ Cam was first discovered by Khruslov (2006) through the data of Northern Sky Variability Survey (NSVS, Woźniak et al. (2004)). Khruslov (2006) has given that the light curve of this binary star is EW-type and the orbit period is 0.43784 days. At present, the photometric solution and the orbit period investigation of OQ Cam have not been published. In this paper, we analyzed the four-color light curves and orbital period variation of OQ Cam for the first time.

2 CCD PHOTOMETRIC OBSERVATION

We have observed OQ Cam using 60 cm Ningbo Bureau of Education and Xinjiang Observatory Telescope (NEXT) and the Weihai Observatory 1.0-m telescope of Shandong University (WHOT) (Hu et al. 2014) from 2018 to 2019. The CCDs of NEXT and WHOT both have 2k×2k pixels. Their field of views are $22' \times 22'$ and $12' \times 12'$, respectively. The standard Johnson-Cousin-Bessel B,V,R_c,I_c filters have been used. The details of the observations are listed in Table 1. The variable, comparison and check stars
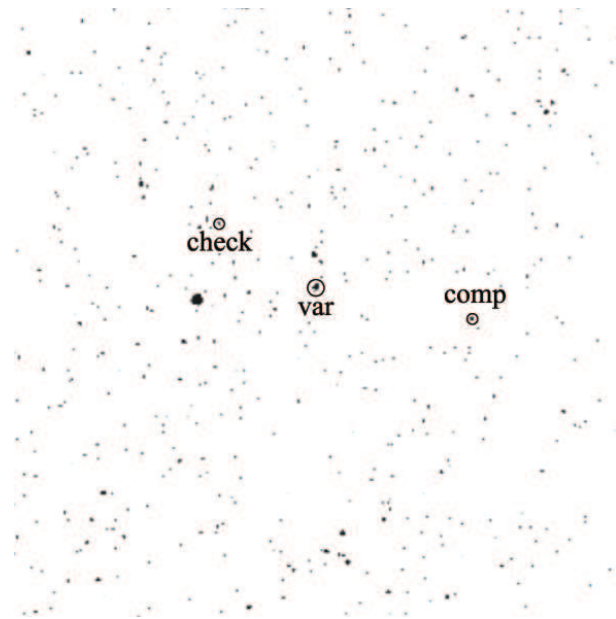
Fig. 1 The image of OQ Cam in B band observed by NEXT. The "var" refers to the variable star, the "comp" refers to the comparison star and "check" refers to the check star.

Table 1 Observation Information

Date	Filter and exposure time	Type	Telescope
2018.12.24	$B60sV40sR_c50sI_c40s$	minimum	NEXT
2018.12.25	$B30sV20sR_c20sI_c20s$	minimum	NEXT
2018.12.26	$B20sV5sR_c5sI_c5s$	light curve	NEXT
2019.11.01	$V10s$	minimum	WHOT

are shown in Figure 1, and some of their information is displayed in Table 2.

We used the C-Munipack[1] program to process the CCD data. The bias and flat corrections have been conducted for all images. The aperture photometry and differential photometry were used to reduce the CCD data. Then, the magnitude differences between the variable and comparison stars, and those between the comparison and check stars were determined. The four-color light curves observed on 2018 December 26 are plotted in Figure 2. The x-axis is the Heliocentric Julian Date (HJD), and the y-axis is the magnitude difference. From the light curves, we can find that the light curves change continuously and the secondary minima are as deep as the primary minima. The magnitude differences between the comparison and check stars are plain, suggesting that both the comparison and check stars are not variable stars.

3 PHOTOMETRIC SOLUTIONS

According to the complete light curves of OQ Cam, the secondary minima are almost as deep as the primary mini-

---

[1] *http://c-munipack.sourceforge.net/*

Table 2 Details of the Variable, Comparison and Check Stars

Star	Name	R.A.	Decl.	J(mag)	H(mag)	K(mag)
Variable star	OQ Cam	$03^h 33^m 34.32^s$	$+64° 16' 46.2''$	9.638	9.351	9.292
Comparison star	2MASS J03324359+6415410	$03^h 32^m 43.59^s$	$+64° 15' 41.0''$	9.362	8.725	8.503
Check Star	2MASS 03340661+6418584	$03^h 34^m 06.61^s$	$+64° 18' 58.4''$	8.663	7.833	7.605
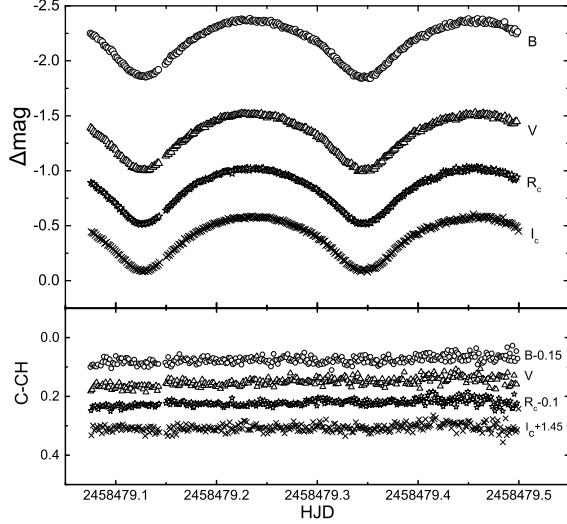
Fig. 2 The figure displays the light curves of OQ Cam observed by NEXT on 2018 December 26. The bottom of this figure is the magnitude difference between the comparison and check stars. "C" and "CH" refer to the comparison and check stars, respectively.

Table 3 Photometric Results

Parameter	Value	Error
$g_1 = g_2$	0.32	Assumed
$A_1 = A_2$	0.5	Assumed
T_1(K)	5676	Assumed
T_2(K)	5721	6
$q(M_2/M_1)$	0.479	0.007
Ω_{in}	2.835	–
Ω_{out}	2.548	–
$\Omega_1 = \Omega_2$	2.777	0.014
i	73.1	0.1
$(L_1/L_1 + L_2)_B$	0.647	0.001
$(L_1/L_1 + L_2)_V$	0.650	0.001
$(L_1/L_1 + L_2)_{Rc}$	0.652	0.001
$(L_1/L_1 + L_2)_{Ic}$	0.653	0.001
r_1(pole)	0.428	0.001
r_1(side)	0.457	0.002
r_1(back)	0.489	0.002
r_2(pole)	0.307	0.005
r_2(side)	0.322	0.007
r_2(back)	0.363	0.012
f	20.2%	4.9%

mum, indicating that OQ Cam is a typical EW-type binary star. The Wilson-Devinney (W-D) program (Wilson 1979, 1990; Wilson & Devinney 1971) was applied to model the light curves. Gaia DR 2 (Gaia Collaboration et al. 2016, 2018) has determined a surface temperature of 5676 K for OQ Cam, which is treated as the temperature of the primary star. This surface temperature is estimated through the approach of Priam algorithm according to the Gaia three-band photometry with an accuracy of about 324 K in the range 3000 K to 10 000 K (Andrae et al. 2018). The gravity-darkening coefficients and the bolometric albedos were set as $g_{1,2}= 0.32$ and $A_{1,2} = 0.5$ due to the convective envelopes (Lucy 1967). The bolometric and bandpass limb-darkening coefficients were chosen from van Hamme (1993)'s table.

No investigation has been carried out for OQ Cam, hence we used the method of q-search to determine its mass ratio. The details are as follows: the mass ratio was fixed at a range from 0.1 to 10, and the step length is 0.1. Then we can obtain a series of convergent solutions. In the processing of running the program, orbital inclination, the temperature of secondary star, the luminosity of the primary star in BVR_cI_c bands, and the dimensionless potential of the primary star are adjustable parameters. The sum square of residuals versus mass ratio is shown

in Figure 3 (in this figure, we only show the range from 0.2 to 2.5). From the figure, we can find when the mass ratio is 0.4, the sum square of residuals is the smallest. So this value was set as the original mass ratio and an unfixed value. By running the W-D code, the final results were obtained and are shown in Table 3. All the errors in Table 3 are not real ones but only fitting errors computed by the WD program, which are underestimated (Prsa & Zwitter 2005). If one wants to obtain the real errors, Bayesian modeling with Markov Chain Monte Carlo (MCMC) should be applied to model the light curves of eclipsing binaries. The fitting curve is shown in the top panel of Figure 4, and the $O - C$ residuals are shown in the bottom panel. Very flat $O - C$ residuals indicate that the theoretical light curves fit the observed light curves very well. The light curve is symmetric, no spot was needed. In addition, we have searched for the third light, but the value is always negative, so no third light was detected.

4 ORBITAL PERIOD INVESTIGATIONS

A total of 29 minimum moments have been collected from the literatures and our observation data. In which, 22 minimum moments were observed by CCD, and 7 were observed by photoelectric photometer (PE). The time range of these 29 minimum moments is from 1999 to 2019. Based on these minima, we analyzed the orbital period change of OQ Cam. All the minimum moments are listed in Table 4. At first, the $O - C$ values were calculated using
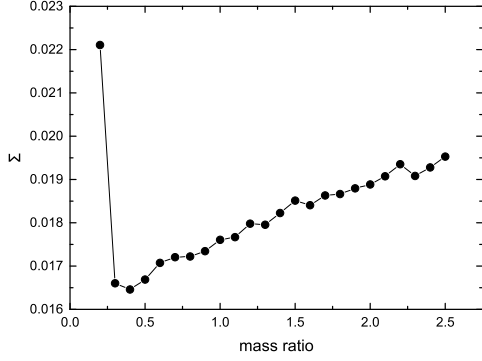
Fig. 3 This figure displays the sum square of residuals Σ versus mass ratio q of OQ Cam.
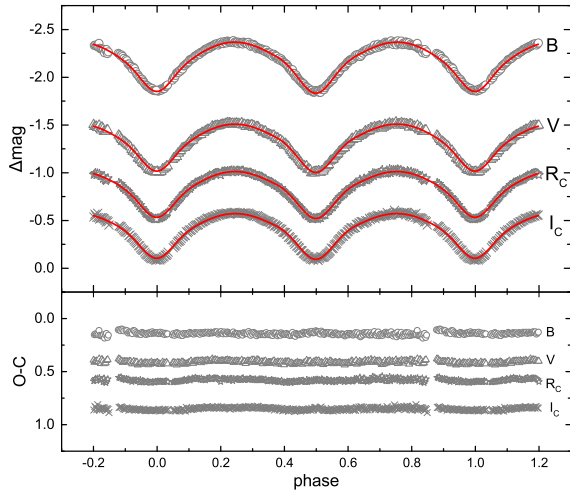
Fig. 4 This figure displays the observed light curves and fitting curves in $B, V, R_c,$ I$_c$ bands of OQ Cam, and the values of $O - C$ are shown in the bottom.

the following linear ephemeris:

$$\mathrm{Min(HJD)} = 2458479.12807 + 0.^{\mathrm{d}}43784 \times E. \quad (1)$$

Then, a linear correction was applied to Equation (1), and a revised linear ephemeris was determined as follows:

$$\begin{aligned} \mathrm{Min(HJD)} = &245879.12127(\pm0.00182) \\ &+ 0.4378401(\pm0.0000004) \times E. \end{aligned} \quad (2)$$

Using this ephemeris, the final $O - C$ values were calculated. The relationship between epoch and $O - C$ is shown in Figure 5. Then we used the least square method to fit the values of $O - C$ and determined the following equation:

$$\begin{aligned} \mathrm{Min(HJD)} \ = \ &2458479.12706(\pm0.00048) \\ &+ 0.4378435(\pm0.0000002) \times E \\ &+ 2.64(\pm0.15) \times 10^{-10} \times E^2. \end{aligned} \quad (3)$$
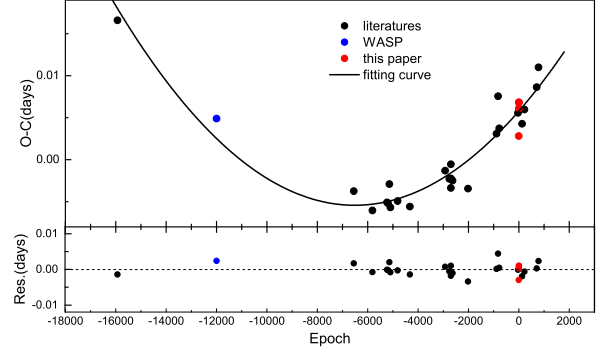
Fig. 5 This figure displays the $O - C$ values of OQ Cam, the black line respects the fitting curve of Equation (2). The residuals are shown in the bottom.
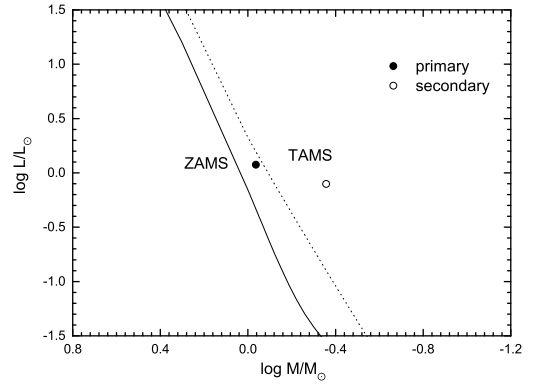
Fig. 6 This figure displays M-L diagram. The solid circle refers to the primary star and hollow circle refers to the secondary star. The solid and dashed lines represent ZAMS and TAMS, respectively.

The corresponding fitting curve labeled by black line is displayed in Figure 5. According to Equation (3), the orbital period exhibits a long term increasing, and the rate is $dP/dt = 4.40(\pm0.25) \times 10^{-7}$ d yr^{-1}.

5 DISCUSSION

According to the results of the photometric solutions, OQ Cam is proven to be a shallow contact binary star with a contact degree of 20.2% and a mass ratio of 0.479. Moreover, the temperature difference between two components is 45K, indicating the binary is in thermal contact. By analyzing all minima, it is found that the orbital period manifests a long term increasing with a rate of 4.40×10^{-7} d yr^{-1}. Like II UMa (Zhou et al. 2016), NO Cam (Zhou et al. 2017), TYC 1337–1137–1 (Liao et al. 2017), this can be explained by mass transfer from the less massive component to the more massive one. According to the temperature of the primary star, its corresponding

Table 4 The Minimum Moments of OQ Cam

JD (Hel.) 2400000+	Error	Method	Min.	Epoch	$O-C$	Residuals	Ref.
51501.7180	-	CCD	p	–15936.0	–0.0166	–0.0014	(1)
53225.7017	0.0010	CCD	s	–11998.5	–0.0049	0.0024	(2)
55609.2946	0.0002	PE	s	–6554.5	–0.0037	0.0017	(3)
55932.6372	0.0003	CCD	p	–5816.0	–0.0061	–0.0008	(4)
56187.4611	0.0001	PE	p	–5234.0	–0.0051	–0.0001	(5)
56205.8503	0.0001	CCD	p	–5192.0	–0.0052	–0.0002	(6)
56227.9635	0.0005	CCD	s	–5141.5	–0.0029	0.0020	(7)
56246.3500	0.0001	CCD	s	–5099.5	–0.0057	–0.0008	(8)
56371.3541	0.0005	CCD	p	–4814.0	–0.0049	–0.0003	(9)
56585.8951	0.0010	CCD	p	–4324.0	–0.0056	–0.0014	(10)
57196.4674	0.0005	CCD	s	–2929.5	–0.0013	0.0007	(11)
57270.4614	0.0001	PE	s	–2760.5	–0.0023	–0.0006	(12)
57296.2957	0.0010	PE	s	–2701.5	–0.0005	0.0010	(12)
57296.5118	0.0006	PE	p	–2701.0	–0.0034	–0.0018	(12)
57298.4832	0.0041	PE	s	–2696.5	–0.0022	–0.0007	(12)
57327.3804	0.0003	PE	s	–2630.5	–0.0025	–0.0011	(12)
57595.5565	0.0002	CCD	p	–2018.0	–0.0035	–0.0034	(11)
58090.7602	0.0002	CCD	p	–887.0	0.0031	0.0002	(13)
58117.4729	0.0002	CCD	p	–826.0	0.0076	0.0044	(14)
58136.5151	0.0002	CCD	s	–782.5	0.0038	0.0005	(14)
58465.5538	0.0002	CCD	p	–31.0	0.0056	–0.0001	(14)
58477.3727	0.0023	CCD	p	–4.0	0.0028	–0.0030	(15)
58478.2524	0.0023	CCD	p	–2.0	0.0068	0.0011	(15)
58479.1281	0.0003	CCD	p	0.0	0.0068	0.0010	(15)
58479.3463	0.0003	CCD	s	0.5	0.0061	0.0003	(15)
58534.2954	0.0003	CCD	p	126.0	0.0043	–0.0020	(14)
58576.3278	0.0004	CCD	p	222.0	0.0060	–0.0006	(14)
58789.1207	0.0001	CCD	p	708.0	0.0086	–0.0003	(15)
58821.3043	0.0002	CCD	s	781.5	0.0110	0.0024	(14)

(1)Khruslov (2006); (2)This paper (WASP); (3)Hubscher & Lehmann (2012); (4)Diethelm (2012); (5)Hubscher & Lehmann (2013); (6)Nelson (2013); (7)Diethelm (2013); (8)Hoňková et al. (2013); (9)Corfini et al. (2014); (10)Diethelm (2014); (11)Jurysek et al. (2017); (12)Hubscher (2017); (13)Nelson (2018); (14)*http://var2.astro.cz/brno/protokoly.php*; (15)This paper.

Table 5 W-subtype Shallow Contact Binaries with Increasing Orbital Period

Star	Period (d)	q	$f(\%)$	T_1(K)	T_2(K)	dp/dt (d yr^{-1})	Reference
AR Boo	0.344874	0.382	12.3	5100	5398	2.68×10^{-7}	Lee et al. (2009)
AD Cnc	0.282729	0.770	8.3	4790	5000	4.94×10^{-7}	Qian et al. (2007)
FZ Ori	0.399986	0.860	2	5940	5983	2.28×10^{-8}	Prsa & Zwitter (2005)
RZ Com	0.338507	0.425	20.1	4900	5000	3.97×10^{-8}	He & Qian (2008)
FP Lyn	0.359085	0.867	13.4	5683	5909	4.19×10^{-7}	Michel et al. (2019)
FV CVn	0.315365	0.930	4.6	5120	5470	7.70×10^{-7}	Michel et al. (2019)
PS Vir	0.289806	0.305	14.4	5800	5976	1.26×10^{-7}	Yuan et al. (2018)
TY UMa	0.354548	0.396	13.4	6229	6250	5.18×10^{-7}	Li et al. (2015)
J140533.33+114639.1	0.225123	0.645	7.9	4563	4680	2.09×10^{-7}	Zhang et al. (2018)
V509 Cam	0.350347	0.364	10	5662	5902	3.96×10^{-8}	Li et al. (2019)
AE Phe	0.362375	0.392	14.6	5940	5983	6.17×10^{-8}	He et al. (2009)

(1) $q = M_2/M_1$; (2) The subscript 1, 2 represent the massive and less massive star, respectively.

spectral type is G5 (Cox 2000). Assuming the primary star is a main-sequence star and based on Cox (2000), the mass of the primary star can be estimated to be $M_1 = 0.92M_\odot$. The mass of the secondary star is calculated: $M_2 = M_1 \times 0.473 = 0.44M_\odot$. Using the following equation:

$$\frac{dM_2}{dt} = \frac{M_1 M_2}{3P(M_1 - M_2)} \times \frac{dP}{dt}, \tag{4}$$

the mass transfer rate was calculated to be $dM_2/dt = 2.82 \times 10^{-7} M_\odot$ yr^{-1}.

We also calculated the distance between the two component stars based on their masses and gained $a = 2.69R_\odot$ according to $M_1 + M_2 = 0.0134a^3/P^2$. The radii of the primary and secondary stars can be computed to be $R_1 = (r_{1\text{pole}} \cdot r_{1\text{side}} \cdot r_{1\text{back}})^{1/3} \cdot a = 1.23R_\odot$ and $R_2 = (r_{2\text{pole}} \cdot r_{2\text{side}} \cdot r_{2\text{back}})^{1/3} \cdot a = 0.89R_\odot$, respectively. The luminosities of the primary and secondary stars are $L_1 = (T_1/T_\odot)^4 \cdot (R_1/R_\odot)^2 = 1.19L_\odot$ and $L_2 = (T_2/T_\odot)^4 \cdot (R_2/R_\odot)^2 = 0.79L_\odot$ respectively. To intuitively reflect the evolution of the two stars, we drew the mass-luminosity (M-L) diagram as shown Figure 6. "ZAMS" and "TAMS"

refer to zero-age main sequence and terminal-age main sequence, respectively, which are constructed based on the binary evolution code provided by Hurley et al. (2002). From the M-L diagram, the primary star is located between the ZAMS and TAMS, meaning that it is a main sequence star, while the secondary star is located above the TAMS, indicating that the secondary star is at an advanced evolutionary stage. The evolutionary stages of the two components are similar with those of other W-type contact binaries. Table 5 shows some W-type shallow contact binaries with increasing period. As seen in Table 5, OQ Cam has a similar orbital period increasing rate to the other stars.

OQ Cam shows a long term increasing in orbit period and its mass ratio is 0.479. This agrees with the result that for the W-type contact stars with $q>0.4$, their periods show a long term increasing, while $q<0.4$, their periods show a long term decreasing (Qian 2001). Due to the increasing period, the distance between the primary and secondary stars will be increasing. Further, OQ Cam may evolve from the present shallow contact stage to the non-contact stage. This is consistent with the thermal relaxation oscillation theory (Lucy 1976; Flannery 1976; Robertson & Eggleton 1977). Therefore, it may be a potential candidate to confirm the thermal relaxation oscillation theory. However, further observations and investigations are needed.

References

Andrae, R., Fouesneau, M., Creevey, O., et al. 2018, A&A, 616, A8

Awadalla, N. S., & Hanna, M. A. 2005, Journal of Korean Astronomical Society, 38, 43

Binnendijk, L. 1970, Vistas in Astronomy, 12, 217

Binnendijk, L. 1977, Vistas in Astronomy, 21, 359

Bradstreet, D. H., & Guinan, E. F. 1994, in ASPC Series, 56, Interacting Binary Stars, ed. A. W. Shafter, 228

Butters, O. W., West, R. G., Anderson, D. R., et al. 2010, A&A, 520, L10

Corfini, G., Aceti, P., Arena, C., et al. 2014, Information Bulletin on Variable Stars, 6094, 1

Cox, A. N. 2000, Introduction, ed. A. N. Cox, Allen's Astrophysical Quantities (New York: AIP Press; Springer), 1

Diethelm, R. 2012, Information Bulletin on Variable Stars, 6011, 1

Diethelm, R. 2013, Information Bulletin on Variable Stars, 6042, 1

Diethelm, R. 2014, Information Bulletin on Variable Stars, 6093, 1

Eker, Z., Demircan, O., Bilir, S., & Karataş, Y. 2006, MNRAS, 373, 1483

Flannery, B. P. 1976, ApJ, 205, 217

Gaia Collaboration, Prusti, T., de Bruijne, J. H. J., et al. 2016, A&A, 595, A1

Gaia Collaboration, Brown, A. G. A., Vallenari, A., et al. 2018, A&A, 616, A1

Gazeas, K. D., & Niarchos, P. G. 2006, MNRAS, 370, L29

He, J.-J., & Qian, S.-B. 2008, ChJAA (Chin. J. Astron. Astrophys.), 8, 465

He, J. J., Qian, S. B., Fernández Lajús, E., et al. 2009, AJ, 138, 1465

He, J. J., Qian, S. B., & Soonthornthum, B. 2016, AJ, 152, 120

Hilditch, R. W., King, D. J., & McFarlane, T. M. 1989, MNRAS, 237, 447

Hoňková, K., Juryšek, J., Lehký, M., et al. 2013, Open European Journal on Variable Stars, 160, 1

Hu, S.-M., Han, S.-H., Guo, D.-F., & Du, J.-J. 2014, RAA (Research in Astronomy and Astrophysics), 14, 719

Hubscher, J. 2017, Information Bulletin on Variable Stars, 6196, 1

Hubscher, J., & Lehmann, P. B. 2012, Information Bulletin on Variable Stars, 6026, 1

Hubscher, J., & Lehmann, P. B. 2013, Information Bulletin on Variable Stars, 6070, 1

Hurley, J. R., Tout, C. A., & Pols, O. R. 2002, MNRAS, 329, 897

Juryšek, J., Hoňková, K., Šmelcer, L., et al. 2017, Open European Journal on Variable Stars, 179, 1

Khruslov, A. V. 2006, Peremennye Zvezdy Prilozhenie, 6, 11

Kim, H.-W., Kim, C.-H., Song, M.-H., et al. 2016, Journal of Astronomy and Space Sciences, 33, 185

Lee, J. W., Youn, J.-H., Lee, C.-U., et al. 2009, AJ, 138, 478

Li, K., Hu, S. M., Guo, D. F., et al. 2015, AJ, 149, 120

Li, K., Xia, Q.-Q., Liu, J.-Z., et al. 2019, RAA (Research in Astronomy and Astrophysics), 19, 147

Liao, W. P., Qian, S. B., Soonthornthum, B., et al. 2017, PASP, 129, 124204

Liu, L., Qian, S. B., & Xiong, X. 2018, MNRAS, 474, 5199

Lucy, L. B. 1967, ZAp, 65, 89

Lucy, L. B. 1976, ApJ, 205, 208

Michel, R., Xia, Q.-Q., & Higuera, J. 2019, RAA (Research in Astronomy and Astrophysics), 19, 099

Nelson, R. H. 2013, Information Bulletin on Variable Stars, 6050, 1

Nelson, R. H. 2018, Information Bulletin on Variable Stars, 6234, 1

Prasad, V., Pandey, J. C., Patel, M. K., et al. 2014, Ap&SS, 353, 575

Prsa, A. & Zwitter, T. 2005, ApJ, 628, 426

Qian, S. 2001, MNRAS, 328, 635

Qian, S.-B., He, J.-J., Zhang, J., et al. 2017, RAA (Research in Astronomy and Astrophysics), 17, 087

Qian, S. B., Yuan, J. Z., Soonthornthum, B., et al. 2007, ApJ, 671, 811

Qian, S. B., Wang, J. J., Zhu, L. Y., et al. 2014, ApJS, 212, 4

Robertson, J. A., & Eggleton, P. P. 1977, MNRAS, 179, 359

Roxburgh, I. W. 1965, AJ, 70, 330

Stepień, K. 2006, Acta Astronomica, 56, 347

Stepień, K., & Gazeas, K. 2012, Acta Astronomica, 62, 153

van Hamme, W. 1993, AJ, 106, 2096

Wilson, R. E. 1979, ApJ, 234, 1054

Wilson, R. E. 1990, ApJ, 356, 613

Wilson, R. E., & Devinney, E. J. 1971, ApJ, 166, 605

Woźniak, P. R., Vestrand, W. T., Akerlof, C. W., et al. 2004, AJ, 127, 2436

Yuan, H.-Y., Dai, H.-F., & Yang, Y.-G. 2018, RAA (Research in Astronomy and Astrophysics), 18, 078

Yildiz, M., & Doğan, T. 2013, MNRAS, 430, 2029

Zhang, B., Qian, S.-B., Michel, R., Soonthornthum, B., & Zhu, L.-Y. 2018, RAA (Research in Astronomy and Astrophysics), 18, 030

Zhang, X.-D., Qian, S.-B., & Liao, W.-P. 2020, MNRAS, 492, 4112

Zhao, E., Qian, S., Li, L., et al. 2014, New Astron., 26, 112

Zhou, X., Qian, S. B., Zhang, J., Zhang, B., & Kreiner, J. 2016, AJ, 151, 67

Zhou, X., Qian, S., & Zhang, B. 2017, PASJ, 69, 37